

"Nanoscale Detectors: Proof of Concept"

Final Progress Report

Russell Giannetta, Ilesanmi Adesida

November 23, 1998

U.S. Army Research Office

Contract/Grant No. G-DAAH04-95-1-0618

University of Illinois at Urbana-Champaign
Champaign, Illinois

APPROVED FOR PUBLIC RELEASE;

DISTRIBUTION UNLIMITED.

THE VIEWS, OPINIONS, AND/OR FINDINGS CONTAINED IN THIS REPORT ARE THOSE OF THE AUTHORS AND SHOULD NOT BE CONSTRUED AS AN OFFICIAL DEPARTMENT OF THE ARMY POSITION, POLICY, OR DECISION, UNLESS SO DESIGNATED BY OTHER DOCUMENTATION.

19981228 071

REPORT DOCUMENTATION PAGE

Form Approved
OMB NO. 0704-0188

Public reporting burden for this collection of information is estimated to average 1 hour per response, including the time for reviewing instructions, searching existing data sources, gathering and maintaining the data needed, and completing and reviewing the collection of information. Send comment regarding this burden estimate or any other aspect of this collection of information, including suggestions for reducing this burden, to Washington Headquarters Services, Directorate for Information Operations and Reports, 1215 Jefferson Davis Highway, Suite 1204, Arlington, VA 22202-4302, and to the Office of Management and Budget, Paperwork Reduction Project (0704-0188), Washington, DC 20503.

1. AGENCY USE ONLY (Leave blank)		2. REPORT DATE Nov. 23, 1998		3. REPORT TYPE AND DATES COVERED Final Report	
4. TITLE AND SUBTITLE Nanoscale Thermoelectric Detectors: Proof of Concept:				5. FUNDING NUMBERS DAAH04-95-1-0618	
6. AUTHOR(S) Russell Giannetta (PI) Ilesanmi Adesida					
7. PERFORMING ORGANIZATION NAMES(S) AND ADDRESS(ES) Dept. of Physics, Electrical & Computer Engineering University of Illinois At Urbana/Champaign Urbana, IL 61801				8. PERFORMING ORGANIZATION REPORT NUMBER	
9. SPONSORING / MONITORING AGENCY NAME(S) AND ADDRESS(ES) U.S. Army Research Office P.O. Box 12211 Research Triangle Park, NC 27709-2211				10. SPONSORING / MONITORING AGENCY REPORT NUMBER ARO 34390.1-PH	
11. SUPPLEMENTARY NOTES The views, opinions and/or findings contained in this report are those of the author(s) and should not be construed as an official Department of the Army position, policy or decision, unless so designated by other documentation.					
12a. DISTRIBUTION / AVAILABILITY STATEMENT Approved for public release; distribution unlimited.				12 b. DISTRIBUTION CODE	
13. ABSTRACT (Maximum 200 words) The conduction and thermopower of several different low temperature, high mobility mesoscopic GaAs devices has been studied. Quantum point contacts, quantum dots, and finite period lateral superlattices were all studied. We have found evidence for unexpected electronic waveguide-like transport through multiple gate superlattices. Thermoelectric cooling in quantum dot/waveguide structures has been shown to be anomalously large and the thermopower reveals the internal energy level structure of the dot. Both quantum point contacts and quantum dots have been shown to act as bolometers for microwave radiation. New, hybrid low temperature grown/high mobility GaAs devices have been fabricated to permit on-chip picosecond electro-optic signal generation. Tests have been performed to study photoconductive switch performance and to study the response of mesoscopic devices to terahertz bandwidth signals.					
14. SUBJECT TERMS Thermoelectricity, quantum device, nanoscale				15. NUMBER OF PAGES 17	
				16. PRICE CODE	
17. SECURITY CLASSIFICATION OR REPORT UNCLASSIFIED	18. SECURITY CLASSIFICATION OF THIS PAGE UNCLASSIFIED	19. SECURITY CLASSIFICATION OF ABSTRACT UNCLASSIFIED	20. LIMITATION OF ABSTRACT UL		

Introduction

I will report our progress in the following areas into which our studies of nanostructured systems have lead. (1) The observation of conductance steps and thermoelectric stationary points in lateral superlattices. Essentially we have seen evidence for electronic waveguide motion through multiple tunnel barriers. This is our most important and unexpected result. (2) Observations of thermoelectric oscillations in a double bend waveguide. In this case we have seen evidence for single electron charging in the thermopower and have also observed cooling of the electron gas via the Peltier effect. (3) Microwave heating and bolometry using the thermoelectric response of quantum devices. (4) The fabrication of new hybrid low temperature grown / high mobility hybrid structures for picosecond electro-optic measurements and subsequent tests of these devices with a femtosecond laser system. (1-3) have all have been performed with the high mobility two dimensional electron gas (2DEG) at the GaAs/AlGaAs interface. The fabrication has been performed by a graduate students Masud Hannan (now at Intel in Corvallis, Oregon) and more recently Almaz Kuliev under Prof. Adesida's direction. The low frequency measurements were carried out in part by Clark Wagner (graduate student now in ECE) and three REU student during the past summer. The picosecond laser work is currently being performed by a Russian postdoc, Alexander Chernenko. Our source of high mobility GaAs/AlGaAs wafers is Prof. M.R. Melloch from Purdue.

1. Electron Waveguide Motion in Superlattices

The most remarkable and persistent new phenomenon that we have uncovered is the occurrence of waveguide-like conduction through superlattice structures. This was completely unexpected. To provide a background, consider first the electronic transport through a quantum point contact (QPC). The width of the QPC is of order the Fermi wavelength in the 2DEG (typically $0.05 \mu\text{m}$) so that the wavefunction for motion transverse to the direction of current flow is quantized into electric sub-bands of energy spacing $\hbar\omega_0$. The sub-band spacing is related to the curvature of the parabolic potential well transverse to the motion. The wavefunction for motion along the direction of the current flow is essentially free, with parabolic dispersion. By changing the gate voltage on the QPC we can open up successive waveguide conductance channels (waveguide modes) each of which carries a unit of conductance $G=2e^2/h$. [1,2] By adding a magnetic field normal to the 2DEG a magnetic depopulation effect occurs. In a parabolic potential approximation, the effective electron waveguide sub-band energy spacing, $\hbar\omega_0$, is changed by the addition of a magnetic field,

$$(1) \quad \omega^2 = \omega_0^2 + \left(\frac{eB}{m^*c} \right)^2$$

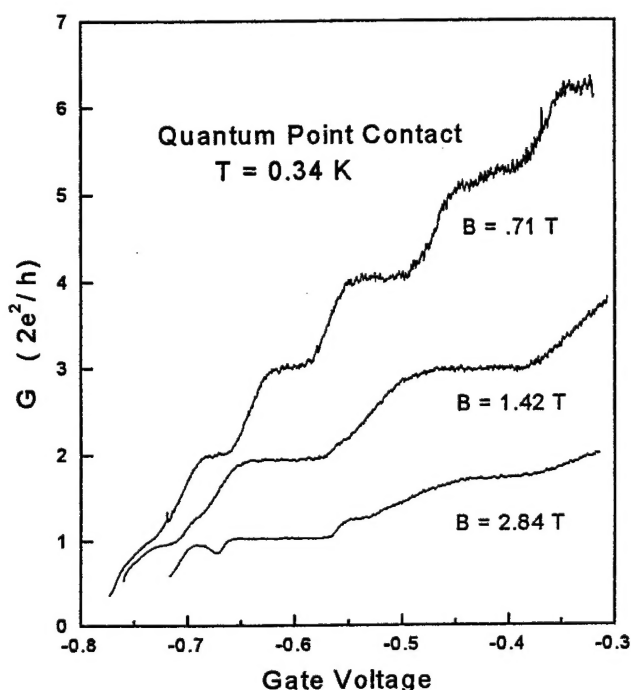
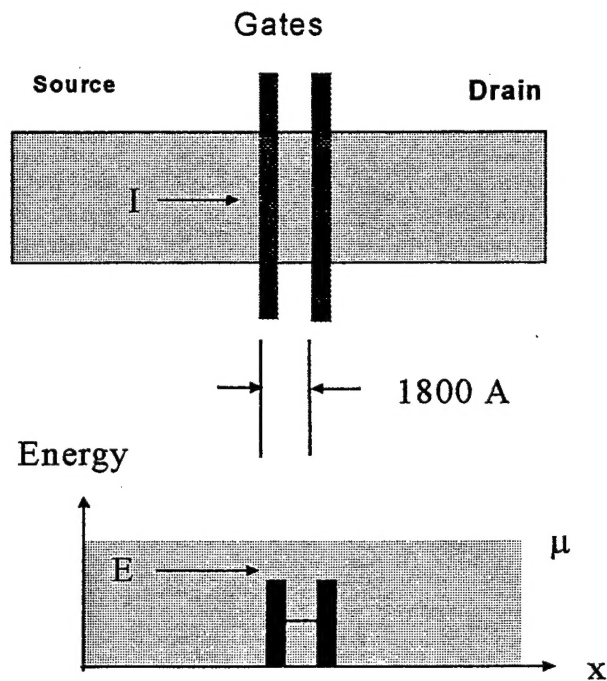


Fig.1. Magnetic depopulation of a quantum point contact.

As B increases both the subband spacing and the effective mass increase, thus requiring larger gate voltages to open successive waveguide channels. The conductance plateaus become increasing wide, as shown in the Fig.1. The plateaus are extremely flat at moderate fields, indicating perfect single mode conduction over a wide range of gate voltage. By measuring the field change required to depopulate a sub-band we can estimate the zero field subband energy spacing at a given gate voltage. We find that at a gate voltage of -0.4 V we have $\hbar\omega_0 = 0.7 \text{ meV}$ which is typical of QPC devices.

The origin of waveguide conduction in a QPC is clear. We now turn to an entirely different geometry: that of a finite lateral superlattice. The simplest version of the superlattice structure that we tested consisted of only 2 gate fingers lying completely across the conducting channel. This is essentially a lateral version of the well-studied resonant tunneling diode. Schematically, the device and its energy landscape looks as shown above in Fig. 2. As the gate potential is changed we would expect to see oscillations in the transmission (conductance) as the chemical potential of the 2DEG becomes close to the top of the potential barriers, then a resonant transmission peak, and then pinch-off. In the actual devices, Schottky gates were patterned across a $3 \mu\text{m}$ wide 2DEG channel. The interleaving gate "fingers" defined a potential modulation with an 1800 \AA period. Several variations on this structure were studied with the number of gate fingers ranging from 2 to 7. Note that the nominal electronic mean was larger than the full width of the superlattice in all cases, so that phase coherent transport processes are expected.

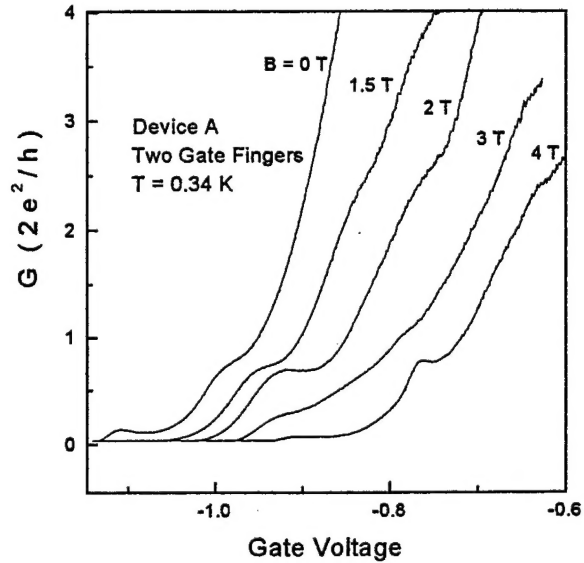
Fig.2. Schematic of two gate lateral superlattice. The lower figure indicates the energy landscape with the resonant state shown between the two energy barriers.



Instead, we observe evidence for waveguide-like motion through this structure as illustrated in Fig.3. We plot conductance versus gate voltage for a variety of different magnetic fields. The plot should be compared to Fig. 1 for the QPC. Note the occurrence of a plateau at $G = .75$ conductance quanta. As the magnetic field is increased the plateau increases in width, much like the magnetic depopulation effect in the QPC. The situation differs from the QPC in that the plateau does not come at an integer conductance step, possibly due to a transmission coefficient less than unity. Moreover, the plateau vanishes for a particular value of the field before reappearing. Despite these differences, our two gate device is largely acting as an electronic waveguide, despite the fact that there exists no obvious conduction path through it. In addition, the $3 \mu\text{m}$ wide 2DEG would normally be expected to support at least 30 conduction channels between the source and drain. It would therefore not show evidence for individual conductance steps at the temperatures investigated here.

Orlov et. al.[3] reported a conductance step and depopulation effects in a wide 2DEG channel gated with a *single* barrier. They attributed the effect to an impurity in the GaAs causing a local distortion of the potential sufficient to permit a natural QPC to form, thus allowing single channel conduction. Although this model is quite plausible and gave a satisfactory explanation of their data, our situation is more complicated since we now have *two* gates present and so the probability of find such a natural, impurity-induced channel through both barriers becomes somewhat less. We pursued two avenues of inquiry from this point (1) tests of devices with a larger number of gates and (2) thermoelectric power measurements to further check for waveguide conduction.

Fig.3 Conductance versus gate voltage for a two finger lateral resonant tunneling diode. Note the presence of a conductance plateau at $G = 3/4$ that becomes more clearly defined at particular values of the magnetic field. Compare to Fig.1 for the magnetic depopulation of the electric sub-band states in a conventional quantum point contact.



Recall that the thermopower in an ideal electron waveguide should exhibit peaks of magnitude,

$$S = \frac{k_B \ln 2}{e n + 1/2} \approx -40 \mu V / \text{Kelvin}, (n=1)$$

as a function of the gate voltage. These peaks are located *between* conductance plateaus where the transmission coefficient is changing most rapidly. The thermopower drops to zero where the QPC conductance exhibits a plateau indicating that only an integral number of conducting channels are open. The thermopower measurement is shown schematically in Fig.4. An ac heating current (typically 50-500 nA) at frequency ω generates temperature oscillations at frequency 2ω on one side of the device. The thermoelectric voltage across the device is then monitored with a lockin amplifier set to detect at 2ω . If we are observing effective waveguide transmission through the superlattice we might also expect behavior in the thermopower similar to that of a QPC.

We performed conductance and thermopower measurements on the 7 gate superlattice. The data is shown in Fig.5. In this case, even in zero magnetic field we observed two clear conductance plateaus, both with $G < 1$, just prior to pinch-off. Although the location with respect to gate voltage varies from device to device, we continue to observe these $G < 1$ plateaus in all of our superlattice structures. Notice that the thermopower is *stationary* at points where the conductance has a plateau. This once again suggests that the superlattice is exhibiting waveguide conduction, even with seven potential barriers.[4] We have now seen this phenomenon in several

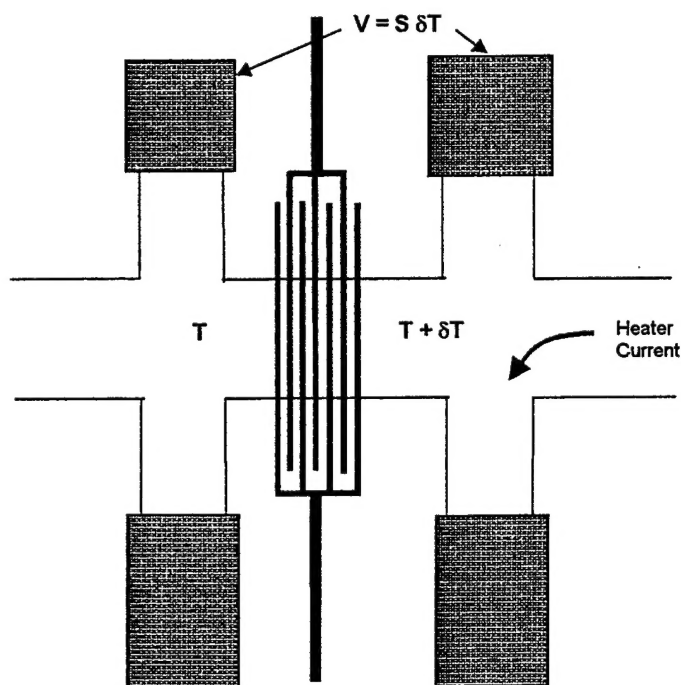


Fig. 4 Thermoelectric power measurement of a superlattice. A current of typically 100 nA generates ohmic heating and a temperature rise in the 2DEG on the right side of the superlattice. Seebeck voltage is generated across the contact pads which is proportional to the thermopower.

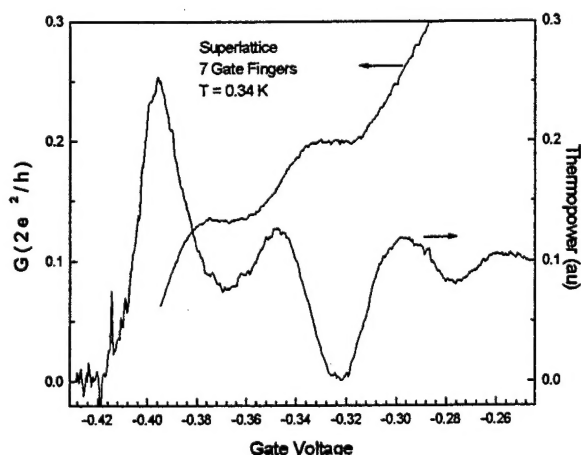


Fig.5. Conductance and thermopower for the 7 gate superlattice. Note the presence of two clear conductance plateaus with corresponding stationary features in the thermopower.

devices and with two different heterostructure layer designs. Although this may result from a fortuitous arrangement of impurities in each case, we feel that something more fundamental, possibly involving electron-electron interactions, may be the root cause.

2. Thermopower and Cooling in Quantum Dots

Thermoelectricity can provide a highly sensitive probe of the transmission characteristics of a quantum device, often exhibiting structure where the conductance fails to show any. In addition, through the basic equations of irreversible heat and charge transport, the presence of a finite thermopower, S , implies the ability to reversibly heat and cool the electron gas with a current. The heat flow is then given by $Q = \Pi I = S T I$ where I is the current passing through the medium and $\Pi = S T$ is the Peltier coefficient. Since the Peltier coefficient for a 2DEG is much less than that of a QPC or a quantum dot, the *mismatch* in electronic heat flow at the interface will result in heating one side of the device and cooling the other via the interaction with the underlying GaAs substrate. These electronic heating and cooling processes will be important whenever moderately large currents (100 nA or more) flow through quantum scale constrictions and so are highly relevant to any practical applications. In addition, the ability to locally cool the 2DEG may have useful signal processing applications.

A quantum dot is a particularly useful device to study Peltier heating and cooling since its thermopower, S , and thus its Peltier coefficient, $\Pi = S T$, can be varied from positive to negative by simply changing the gate voltage defining the dot. This leads to the well known Coulomb blockade oscillations which, in addition to producing a periodic conductance, also produce a periodic, sawtooth behavior in the thermopower. The theoretical curve was first worked out by Bennaker et. al. is shown below.[5] The thermopower (solid line) oscillates as a function of Fermi energy with peak values of order $S = \pm \frac{k_B}{e} \frac{e^2}{2C k_B T}$ where C is the capacitance that

determines the charging energy of the dot. In a sense, the dot is acting like a semiconductor which can be changed from p to n type by changing the gate voltage. Since the ratio of charging energy to thermal energy can become very large for a quantum dot, the thermopower can become much larger than that for a QPC which is in turn much larger than that of the free 2DEG.

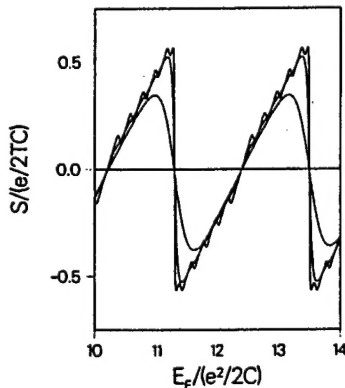


Fig.6. Thermopower oscillations in a quantum dot for successively smaller temperatures relative to the charging energy,

$$k_B T = (0.2, 0.05, 0.01) \frac{e^2}{2C}.$$

From ref.[5].

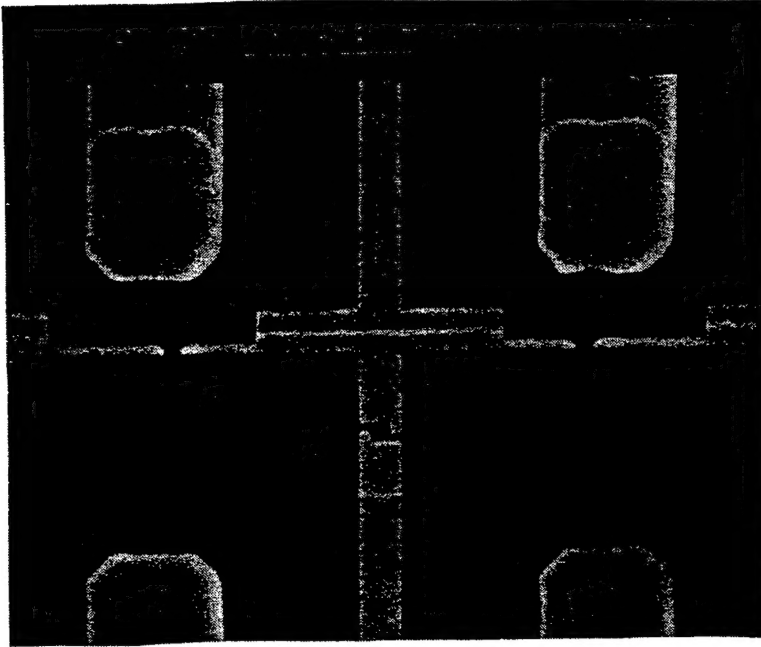


Fig. 7. SEM photograph of quantum dot thermoelectric cooling device. Quantum point contacts are patterned upstream and downstream of the central gate defining the quantum dot.

An SEM photo of the circuit used is shown in Fig. 7. The central device is a hybrid electron waveguide-quantum dot structure. Quantum point contacts are fabricated both upstream and downstream of the device to monitor the electronic temperature of the channel. Using one of the QPC's as a thermometer, we monitor the thermoelectric voltage across it as we sweep the gate voltage of the central quantum dot device.

The Peltier heating and cooling curve is shown in Fig. 8. The downstream 2DEG temperature imbalance ($T_{2DEG} - T_{Lattice} = \delta T$) is monitored by the QPC thermometer. As we sweep the gate voltage of the quantum dot, the temperature imbalance goes from negative to positive reflecting the change in sign of the Peltier coefficient of the quantum dot. While the general effect is unmistakable, the overall size is a mystery. Using the thermopower of the QPC as the coefficient of proportionality between the thermovoltage and the temperature imbalance, Fig. 8 would imply Peltier cooling of over 1.5 Kelvin which is larger than the ambient lattice temperature. In effect, the signal is enormous, suggesting that the simple linear transport theory of the thermoelectric coefficient of a quantum dot does not hold quantitatively. We plan next to use the amplitude of SdH oscillations to measure the absolute temperature of the cooled electrons downstream from the dot. The main point here is that nonequilibrium effects are easily observed in these quantum systems and the effective electronic temperature will dramatically affect their electrical characteristics. Rather little research has been performed on this obviously important and very rich new area.

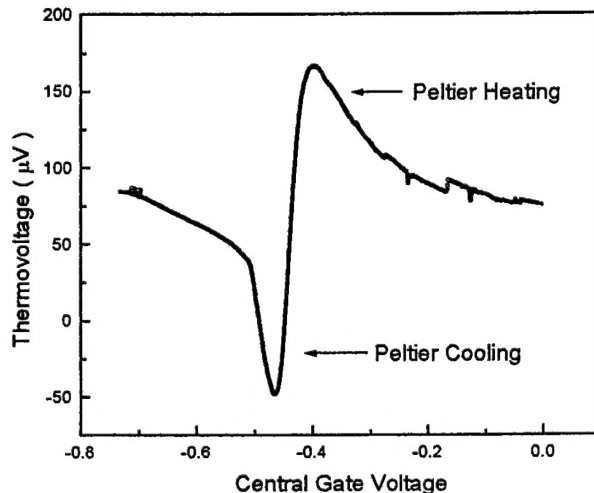
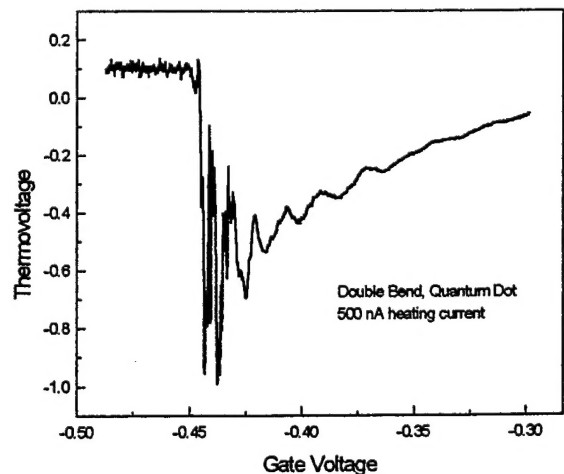


Fig. 8. Peltier heating and cooling of a 2DEG from the quantum dot shown in the previous figure. 500 nA of current is flowing through the device. The thermoelectric voltage is monitored across the downstream quantum point contact.

Fig. 9. Thermopower of double bend quantum dot structure shown in Fig. 7.



If we choose not to drive current through the dot but rather heat the 2DEG to one side of it and measure the thermoelectric voltage across the device, the result is shown in Fig.9. The oscillations for gate voltages above - 0.43 V are due to the presence of the quantum point contacts which serve as entrance arms to the dot. What appears to be high frequency noise as the device approaches pinchoff is actually reproducible signal, as shown in Fig.10. A clear set of higher frequency thermopower oscillations develops. By plotting the oscillation peak index versus voltage, Fig.11 illustrates that these oscillations are very regular with a gate voltage spacing of about 1 meV. This translates into changes of the actual Fermi energy of the dot that are roughly 20 times smaller due to the step down effects of the electrode capacitance and the GaAs layer screening. This fine structure is, we believe, evidence for thermopower oscillations due to the internal electronic energy levels of the dot, which as predicted in ref.[5] and shown in

Fig. 6. To our knowledge only one other group has observed evidence for these internal energy levels.[6] The result again indicates that thermoelectric coefficients can serve as very robust yet sensitive probes of the energy dependent transmission through quantum devices.

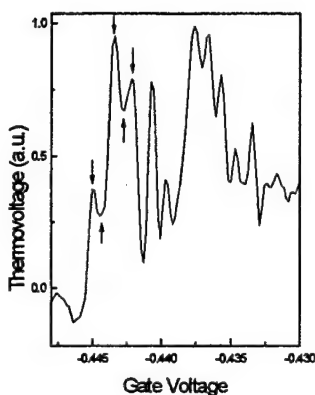
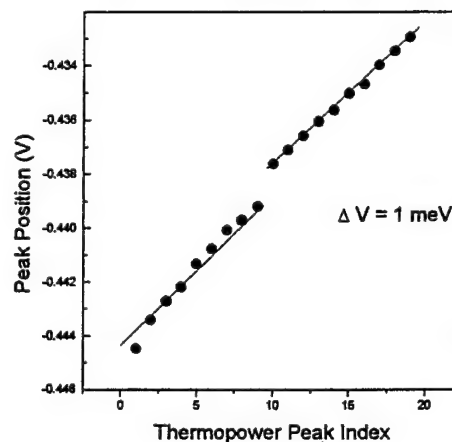


Fig. 11. Peak index versus gate voltage for the fine structure shown in Fig. 10. Slope of the line indicates an average peak spacing of 1 meV.

Fig.10. Enlarged view of fine structure in the thermopower of the double bend quantum dot device. High frequency oscillation peaks and valleys are marked with arrows.



3. Microwave heating in quantum point contacts and quantum dots

The ability to sense the local temperature of the 2DEG leads naturally to the possibility of using quantum dots and point contacts as incoherent detectors of rf and microwave energy. Our measurements consisted of irradiating the device with microwaves in the 1-20 GHz range and measuring the Seebeck voltage across a QPC due to electron heating. The microwave energy was chopped at 17 Hz and the resulting temperature variations of the 2DEG sensed using a lockin amplifier. Figure 12 shows the usual thermoelectric voltage across a QPC due to DC heating of the 2DEG with a current through the channel. The high frequency equivalent, using 5 GHz

microwaves as the source of heating, is shown in Fig. 13. Microwave radiation produces a more clearly defined Seebeck voltage than DC does for reasons that are not clear.

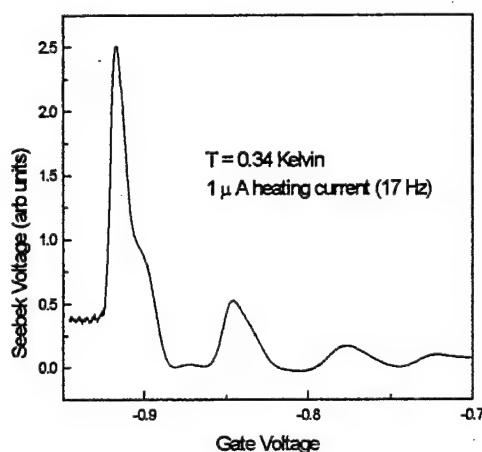
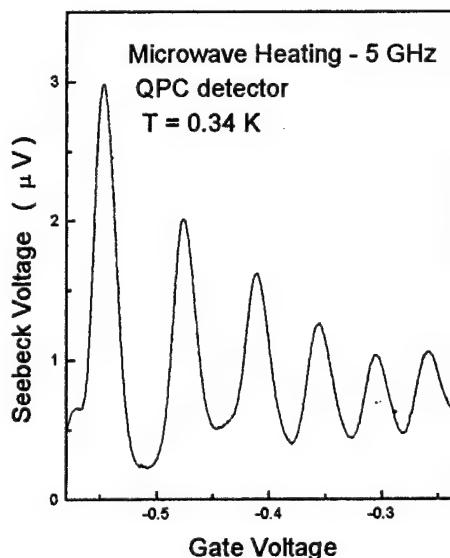


Fig. 12. Thermoelectric voltage across a Quantum Point Contact with 1 microamp heating current to produce a temperature differential.

Fig. 13. Thermoelectric voltage across a QPC due to electron heating by 5 GHz microwave irradiation.



The data is also interesting in that we might not have expected *any* thermopower signal if the 2DEG on both sides of the QPC constriction were heated by the same amount. Apparently a temperature differential develops nonetheless. This may be due to some asymmetry in the coupling of microwaves to different regions of the 2DEG. The more likely explanation is that regions of 2DEG adjacent to an ohmic contact pad (or at least within an inelastic scattering length of the pad) are rapidly thermalized and remain at the lattice temperature. Electrons that are

not near to a contact pad can easily become heated out of equilibrium. In this way a temperature differential can result even though the entire region is illuminated with microwave radiation.

4. Fabrication and testing of picosecond quantum devices.

Two issues will undoubtedly be the basis of a huge amount of future work in mesoscopic systems. The first is simply how mesoscopic transport behavior changes at very high frequencies. How do all the notions of quantized conductance become generalized? As a guide to our high speed experiments we will use an ac generalization of the Landauer-Buttiker result obtained by Fu and Dudley [7]. The ac conductance per waveguide mode at a frequency ω is given by,

$$G(\omega) = \frac{2\pi e^2}{h^2 \omega} \int_{E_F - h\omega}^{E_F} \text{Re} [T(E)T(E + h\omega) + 1 - R(E)R(E + h\omega)] dE$$

with a corresponding expression for the reactance. $T(E)$ and $R(E)$ are the quantum mechanical probability amplitudes for an electron of energy E to be transmitted or reflected from the device. Emission and absorption processes (sometimes called photon-assisted transport) appear in the $h\omega$ factors. The strength of these processes are determined by $T(E)$ and $R(E)$ over a *range* of energies, whereas the DC conductance is determined by T at the Fermi energy alone. This is much like the situation for the thermoelectric coefficients, which are also determined by values of the transmission over a range of energies. When T and R are independent of energy $G(\omega)$ reduces to the usual dc conductance quantization result. Plausible as this picture might seem, our project would be the first experimental test of its validity.

None of the ac effects present in the above formulation will be observable unless incoherent scattering is made negligible. For modern GaAs devices, this implies that frequencies above 50 GHz will be required. This is the upper end of where conventional electronics can operate and the lower end of where electro-optic methods become useful. Our approach has been to integrate the submicron quantum device into a specially fabricated chip that can transmit and receive picosecond electrical pulses produced by the combination of a Ti-sapphire femtosecond pulsed laser and a photoconductive, Auston switch. The layer material has been specifically grown at Purdue by Melloch. It consists of a substrate of 1 micron thick low temperature (LT) grown GaAs that has the short carrier lifetime required to transmit picosecond pulses. On top of this layer is grown high mobility AlGaAs/GaAs heterostructure which is patterned into a mesa as in our previous low frequency devices. Previous attempts by other groups to marry these technologies by connecting the electro-optic switches to the heterostructure components by wires met with enormous mismatch and reflection problems. We felt that by integrated everything onto one chip these problems could be dramatically reduced.

A schematic of our prototype chip is shown below. The 4 arrows are photoconductive (Auston) switches which are essentially metal films separated by a few micron wide gap. A switch is closed with a laser pulse sent through an optical down from room temperature to the

sample stage at cryogenic temperatures. The pulse creates free carriers in the semiconductor between the metal films and temporarily short circuits the coplanar transmission line to a bias voltage pad. The impressed voltage pulse passes down the transmission line, through the quantum device, and is sensed by an output switch which is closed with a delayed laser pulse, thus shunting a time averaged current through the second Auston switch and into a current preamp - lockin amplifier combination. Chopping the laser beam and detecting the change in DC current passed through the output switch as a function of beam delay allows one to effectively map out the received pulse, although not in real time. Multiple photoconductive switches (6 in the actual chip) were placed at 0.5 mm intervals in order to test for attenuation on the stripline and to determine how far away from the device it is possible to apply the laser pulse to minimize heating problems. All the photoconductive switches are connected to external leads to allow for either the application of a bias voltage or connection to a current preamp-lockin combination.

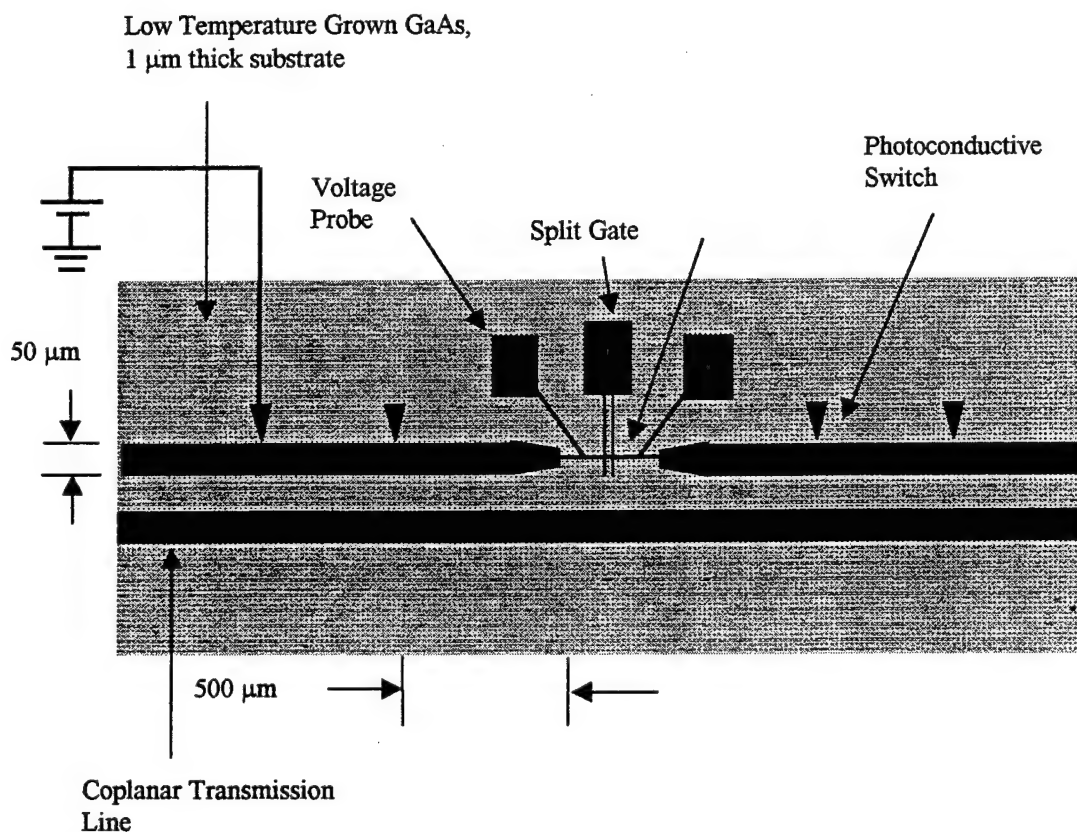


Fig. 13. Schematic of ultra-high frequency test structure for a double barrier lateral resonant tunneling device. Electrodes for the Auston switches are shown as arrows, spaced 0.5 mm apart.

For the submicron device under test we have chosen to use the same finite superlattice design discussed in section 1. This type of device will develop resonant states and will therefore have a much more direct and identifiable effect on a high frequency signal than, for example, a QPC. For example, depending upon the location of the Fermi energy relative to the resonant state (see Fig. 2) it is in principle possible to vary the response of device from purely inductive to purely capacitive, much like a simple LC tank circuit.[7] The change in shape of the transmitted pulse would then be measured by the downstream photoconductive switch. A schematic of the overall experiment is shown in Fig. 14. (The current microstrip design uses two conductors rather than the three shown below on the output, sense lead.) Chip fabrication, setting up the laser system, learning to maximize the efficiency of the optical fibers, and avoiding feedback into the laser itself consumed most of our efforts in recent months. We now have a reasonable efficiency for the conversion of laser pulse energy into an electro-optic signal.

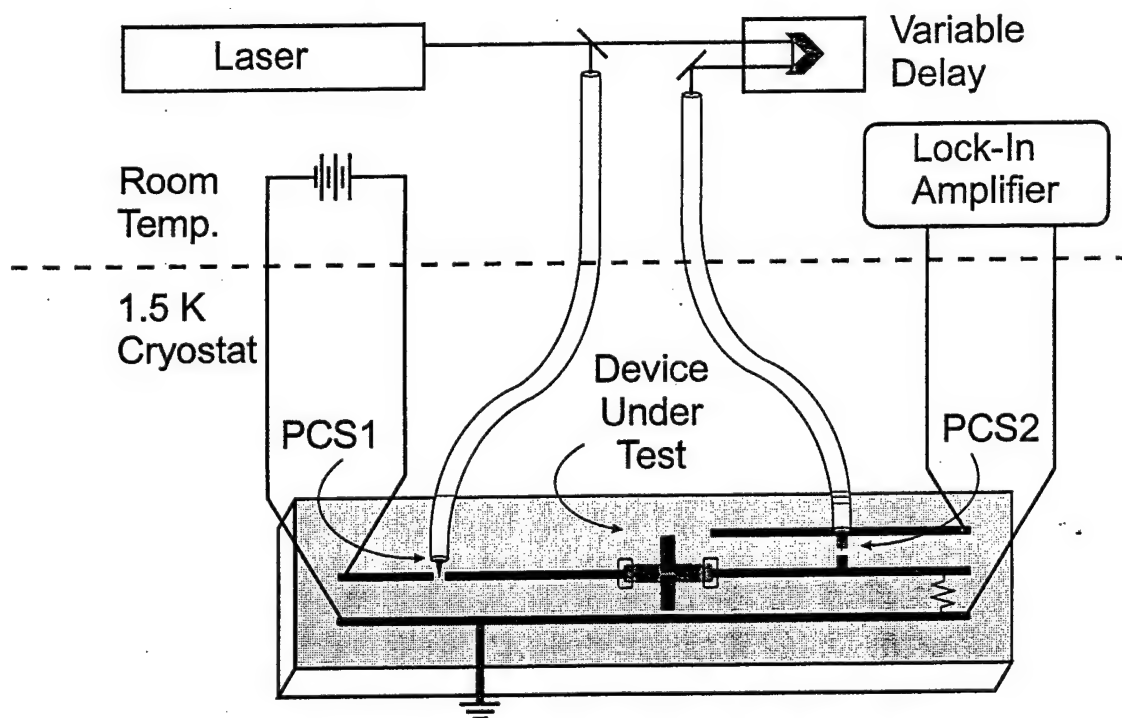


Fig. 14. Experimental schematic for picosecond mesoscopic conductance measurements.

Report Documentation Page (SF298)
(Continuation Sheet)

Our preliminary "received pulse" waveform is shown in Fig. 15. The x-axis is obtained by scanning the room temperature optical delay line and looking for a coincidence when the pulse travelling down the coplanar waveguide finally reaches the output Auston switch. For this scan we used two Auston switches located on the upstream side of the mesoscopic device so as to avoid complications with reflections off the mesoscopic device. It is clear that received pulse is much longer than expected and that we have a good deal of work ahead to obtain clean, picosecond sized pulses. Some of the improvements include (1) each Auston switch will now be plated with resistive nichrome. The intent here is to reduce the possibility of signals rattling back and forth along the switch itself. (2) the ends of the coplanar transmission line have been terminated with thin film nichrome resistors of $66\ \Omega$ to match the transmission line impedance. (3) 60 pF on-chip bias capacitors have been fabricated onto each Auston switch. This serves the same purpose as bias capacitors in any high speed circuit: to provide a local charge reservoir for the Auston switch and to prevent high frequency signals from propagating back toward power supply leads and causing unwanted oscillations and parasitic signals. (4) room temperature compensation for dispersion in the fibers that can cause pulse broadening. We have also tried three microstrip configurations of differing dimension to optimize the pulse shape. We do not believe that the LT GaAs is the problem. A good deal of published work indicates that LT GaAs retains a sufficiently short carrier lifetime even at liquid helium temperatures so as not to degrade the pulse width.

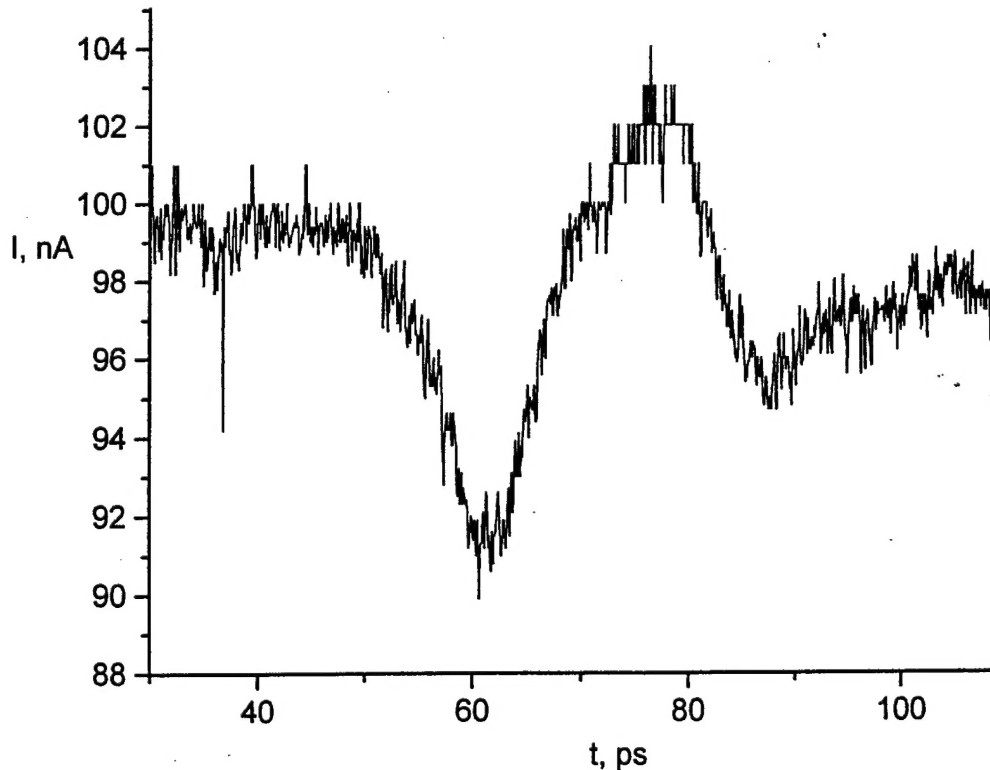
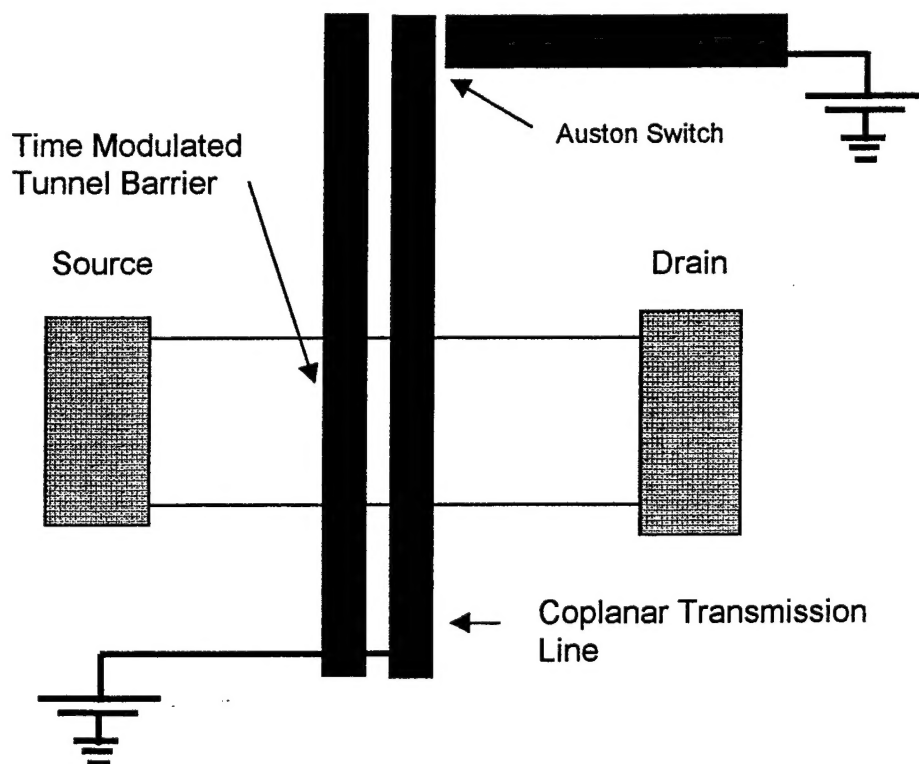


Fig. 15. Receiver Auston switch current output versus optical time delay scan.

The second, and possibly even more interesting issue that arises in high frequency studies is the subject of wavefunction manipulation and control. This is unavoidable when we realize that by simply changing a gate voltage supply we have changed the wavefunction of an electron in a mesoscopic device. Largely unexplored is the issue of how electronic conduction through a mesoscopic device occurs in the presence of arbitrary time-dependent potentials. Some theoretical work by Buttiker and Landauer [8] suggests that entirely new types of conduction would occur when a barrier is modulated at a frequency comparable to the electronic transit time across the barrier. This can be varied by changing the barrier height, but generally the time scales of interest in mesoscale devices would be 1-20 psec. Our initial design for a time-modulated barrier experiment is shown below. In this case, rather than exciting a high speed pulse in the 2DEG, we excite a coplanar stripline that doubles as a Schottky gate across the electron channel. The gate can be given both a dc bias and then pulsed by means of an Auston switch. Our measurements have indicated that a pulse travelling back and forth on this unterminated resonant stripline will take well over 500 psec to decay, giving effectively a pulse train modulation to the potential barrier that an electron sees. We would then simply measure the dc characteristics of the device, but subject to ultra-high speed time modulation. Photon-assisted tunneling is of course once phenomenon that would be expected to occur. This is essential a window of transparency through the barrier that occurs when the barrier height is changed in increments of the barrier modulation sideband energy, $\hbar\omega$, and has now been observed in quantum dots.[9] However, with arbitrary time modulation, a wider variety of wave-packet shaping and manipulation will be possible.



Conclusion

Our project has focused on 4 areas of mesoscopic device behavior. These include (1) The observation of electronic waveguide motion through multiple tunnel barriers. This is our most important and unexpected result. (2) Observations of thermoelectric oscillations in a double bend quantum dot. In this case we have seen evidence for single electron charging and individual quantum dot energy levels in the thermopower. We have also observed cooling of the electron gas via the Peltier effect. We find that the Peltier cooling is unexpectedly large and deserves further attention. (3) Microwave heating and bolometry using the thermoelectric response of quantum devices. In this case, we did not find these devices to be particularly sensitive radiation detectors. (4) The fabrication and testing of new hybrid low temperature grown / high mobility GaAs structures for picosecond electro-optic measurements. We are currently focusing on these high speed measurements with the aid of a UIUC grant of \$100,000 that will run until June 30, 1999. The grant is jointly held by four investigators: R. Giannetta (PI), I. Adesida (co-PI), J. White (co-PI), and P. Phillips (co-PI). These funds have paid the salary for a postdoc - Alexander Chernenko, and will cover the salary of Almaz Kuliev during the spring of 1999, as well as all other laboratory costs.

References

- [1] B.J. van Wees, H. van Houten, C.W.J. Beenakker, J.G. Williamson, L.P. Kouwenhoven, D. van der Marel, and C.T. Foxon, *Phys. Rev. Lett.* **60**, 848, (1988)
- [2] D.A. Wharam, D.J. Thorton, R. Newbury, M. Pepper, H. Ahmed, J.E.F. Frost, D.J. Hasko, D.C. Peacock, D.A. Richie and G.A.C. Jones, *J. Phys. C: Sol. St. Phys.* **21**, L209 (1988)
- [3] A.O. Orlov et. al., *J. Phys.: Condensed Matter* **6**, L349-L354 (1994)
- [4] M. Hannan, R. Grundbacher, P. Fay, I. Adesida, R. W. Giannetta, C. J. Wagner, M. R. Melloch, *Journal of Vacuum Science and Technology B* **15(6)**, 2821, Nov/Dec (1997)
- [5] C.W.J. Beenakker and A.A.M. Staring, *Phys. Rev. B* **46**, 9667 (1992)
- [6] A.S. Dzurak et. al., *Phys. Rev. B.* **55**, R10197 (1997)
- [7] Y. Fu and S. Dudley, *Phys. Rev. Lett.* **70**, 65 (1993)
- [8] M. Buttiker and R. Landauer, *Phys. Rev. Lett.* **49**, 1739 (1982)
- [9] L.P. Kouwenhoven et. al., *Phys. Rev. Lett.* **73**, 3443 (1994)

Report Documentation Page (SF298)
(Continuation Sheet)

Publications from this grant, to date

"Conductance Studies in a Double Bend Quantum Structure", M. Hannan, R. Grundbacher, J. Eom, V. Chandrasekhar, R.W. Giannetta, and I. Adesida, *Superlattices and Microstructures*, **20**, No. 4, 427 (1996)

"Fabrication of Quantum Nanostructures for the Measurement of Thermoelectric Phenomena", M. Hannan, R.W. Giannetta, R. Grundbacher, and I. Adesida, *Journal of Vacuum Science and Technology B*, **14(6)**, 4062 (1996)

"Transport Study in High Mobility GaAs/AlGaAs Lateral Superlattices", M. Hannan, R.W. Giannetta, R. Grundbacher, and I. Adesida, *Journal of Vacuum Science and Technology A* **15**, 1291, (1997)

"Fabrication and Transport Study of Finite Lateral Superlattices ", M. Hannan, R. Grundbacher, P. Fay, I. Adesida, R. W. Giannetta, C. J. Wagner, M. R. Melloch, *Journal of Vacuum Science and Technology B* **15(6)**, 2821, Nov/Dec (1997)

Manuscripts in Preparation

"Thermoelectric Effects in a Double-Bend Waveguide Structure", M. Hannan, I. Adesida, R.W. Giannetta, C.J. Wagner, M.R. Melloch

"Waveguide Conduction in Tunneling Structures", M. Hannan, I. Adesida, R.W. Giannetta, C.J. Wagner, M.R. Melloch

PhD Students Supported

Clark Wagner - graduate student in the Physics department. (June. 1, 1996 - September, 1997)

Masud Hannan - graduate student in Electrical and Computer Engineering (January 20, 1996 - September, 1997) Currently employed at Intel Corporation, Corvallis, Oregon.

Undergraduate Students involved in this research

Daniel Farkas, REU student from Yale University, summer of 1998

Anthony Bak, REU student from Haverford University, summer of 1998

Philip David, REU student from Brown University, summer of 1998

Douglas Dombeck, student at UIUC, currently taking data